# Improving photosynthate allocation dynamic simulations of crops under water stress conditions

Wei Xu[a,b], Wen Zhang[a], Yongqiang Yu[a], Qing Zhang[a,*]

[a] Laboratory of Atmospheric Boundary Layer, Institute of Atmospheric Physics, Chinese Academy of Sciences, Beijing 100029, China

[b] Meteorological Service Center for the Core Areas of the Capital, Beijing Meteorological Service, Beijing 100029, China

Email address: zhangqing@mail.iap.ac.cn

Abstract

Accurately simulating crop photosynthate allocation under water stress is critical for predicting both food security and ecosystem carbon inputs. Current crop models often rely on static or growth-stage-fixed allocation coefficients, which limits their ability to capture the physiological plasticity of crops responding to fluctuating environmental conditions. This study develops a water-driven, stage-dependent carbon allocation scheme within the Agro-C model to better represent crop responses to soil moisture variability. The scheme dynamically adjusts photosynthate allocation coefficients for roots (PR) and leaves (PL), integrates the yellow-to-green leaf ratio (YGR), and incorporates a water stress–induced leaf senescence module. By coupling carbon allocation to both soil moisture and crop development, the approach improves the representation of physiologically regulated allocation processes and enhances the realism of crop simulations. Model evaluation using extensive observation datasets for maize and wheat demonstrates substantial improvements in simulation accuracy, with $R^2$ values reaching 0.77–0.95 for aboveground biomass (AGB) and 0.62–0.83 for belowground biomass (BGB). These results underscore the importance of dynamically representing carbon allocation under water stress and offer an improved framework for simulating carbon–water interactions in agroecosystems.

**Key words:** Crop model, Water stress, Irrigation, photosynthate allocation

## 1. Introduction

The intensification of climate change and increasing pressure on freshwater resources have led to more frequent and severe drought events worldwide (Boretti & Rosa, 2019; Lesk et al., 2016; Vicente-Serrano et al., 2022). Water availability is a key factor regulating crop growth and productivity, as sufficient water promotes biomass accumulation and yield, whereas water deficit can cause substantial reductions (Zlatev & Lidon, 2012). In addition to its direct effects on crop growth, water stress fundamentally alters the allocation of assimilated carbon among plant organs, thereby influencing both plant development and soil carbon inputs.

Maize (*Zea mays L.*) and wheat (*Triticum spp.*), as major global staple crops, are highly sensitive to water availability (Hu et al., 2024; Yan et al., 2025). Water availability strongly influences crop growth by regulating photosynthesis, biomass production, and carbon allocation among plant organs. Under moderate drought, crops often allocate more carbon to roots, thereby promoting root growth and improving water use efficiency (Chen et al., 2019; Oktem, 2008). However, severe water deficit suppresses carbon assimilation, reduces both aboveground and belowground biomass, and ultimately limits yield formation (Khatun et al., 2021; Li et al., 2021). Crop responses also vary with developmental stage and species. For example, wheat generally exhibits enhanced root allocation under mild drought but inhibited root development under severe water stress (Wang et al., 2024; Xue et al., 2003), whereas excessive water conditions, such as waterlogging, impair root function and disrupt carbon allocation (Manghwar et al., 2024). Although recent studies have quantified relationships between water availability and biomass allocation (Xu et al., 2025), incorporating these dynamic responses into crop models remains a major challenge.

Photosynthate allocation is a key process linking carbon assimilation to vegetation growth in terrestrial ecosystem models, whereas it is typically represented using empirical, fixed, or stage-based allocation schemes (Hijmans et al., 1994; Wolf et al., 2003). In the Agricultural Production Systems sIMulator (APSIM), photosynthate allocation among organs is regulated by developmental stage, with

carbon allocated to leaves during the early vegetative growth stage and progressively shifted to stems, reproductive organs, and grains (Keating et al., 2003). In the Carnegie–Ames–Stanford Approach model (CASA) (Field et al., 1995) and the Denitrification-Decomposition (DNDC) model (Li et al., 2011), biomass allocation is largely based on fixed parameters, with the root to shoot ratio (RSR) varying only by vegetation type. In ecosystems, photosynthate allocation is a highly flexible process that responds to changing resource availability, particularly soil moisture conditions, and plays a critical role in regulating both plant growth and soil carbon input. Therefore, developing a mechanistic representation of photosynthate allocation that explicitly accounts for environmental controls is essential for improving model accuracy and physiological realism (Hu et al., 2023).

Moreover, the impacts of water deficit on crops involve multiple aspects of plant growth and development, and it remains challenging to quantitatively and precisely describe water stress in crop models. Most crop models use a water stress coefficient ($K_s$) based on supply–demand balance to adjust assimilate allocation and estimate biomass under stress (Saseendran et al., 2014). For instance, in the APSIM (McCown et al., 1996), CropSyst (Stöckle et al., 1994), and Decision Support System for Agrotechnology Transfer (DSSAT) (Jones et al., 2003), the water stress factor is defined as $K_s = 1 - AT / PT$, where $AT$ is the actual daily water uptake and $PT$ is the potential transpiration. When soil water supply is insufficient to meet the crop's transpiration or evapotranspiration demand, the plant experiences water stress.

However, in contrast, crop water supply primarily depends on root water uptake from the soil (Steudle, 2000). Water transport within the plant is driven by the water potential gradient along the soil–plant–atmosphere continuum, which sustains plant water status and transpiration. Root water uptake is controlled not only by the water potential gradient between soil and roots, but also by root hydraulic conductivity. Thus, plant water uptake capacity is jointly determined by these two factors (Wang et al., 2005; Wang et al., 2013; Yang et al., 2023). In addition, root system architecture, root length density, and the spatial distribution of soil moisture further influence the

efficiency of water acquisition, thereby regulating plant water status and its response to water stress (Javaux et al., 2008). Hence, incorporating root water uptake processes provides a more physiologically meaningful basis for representing water stress in crop models.

Therefore, to better represent crop responses to water stress, this study optimizes the Agro-C model—a biogeophysical framework for simulating crop growth and SOC dynamics (Huang et al., 2009; Yu et al., 2012; Wang et al., 2015; Zhang et al., 2017). Specifically, the optimized model incorporates a process-based root water uptake module to quantify crop water status and introduces a moisture driven dynamic photosynthate allocation scheme that adjusts carbon allocation according to crop developmental stage and water deficit. Focusing on maize and wheat as representative C4 and C3 crops, we aim to: (1) quantify the non-linear responses of leaf and root allocation coefficients (PL and PR) to soil water availability while incorporating a drought-induced leaf senescence module (YGR) to represent declines in photosynthetic capacity; (2) improve the water module of the Agro-C model by integrating root water uptake characteristics, allowing water stress to be represented based on crop physiological responses; and (3) validate the model's performance in capturing carbon trade-offs under extreme water regimes.

## 2. Methods and materials

### 2.1 Data Sources

Based on the datasets used for the meta-analysis by Xu et al. (2025), we further screened studies for model calibration and validation by the following criteria: (i) the study must report belowground biomass (BGB) or aboveground biomass (AGB) for one or more crop growth stages; (ii) the study must provide irrigation amounts or soil moisture conditions throughout the crop growth period; (iii) the study must report fertilizer inputs during the cropping period; and (iv) background and ancillary information such as geographic coordinates, altitude, planting area, planting density, soil type, and bulk density must be described. Meteorological data for the crop

growing period were obtained from *ERA5* (https://cds.climate.copernicus.eu/).

We collected 608 observations of AGB and BGB (315 for maize and 293 for wheat) from 21 published studies, including 198 at maturity and 411 at earlier developmental stages. In 12 studies (maize: 214, wheat: 164), AGB and BGB were recorded at multiple key growth stages, and these data were used for model calibration. In contrast, 9 studies (maize: 101, wheat: 129) reported AGB and BGB only at maturity or vegetative stages, and these data were used for model validation. The geographic distribution of the dataset is shown in Fig. S1.

## 2.2 Simulations of the crop growth responses to the budgets of soil water conditions in the Agro-C model

In Agro-C model, Huang et al. (2009) simulated soil water content based on the principle of soil water balance, using precipitation and actual evapotranspiration at the canopy level. The effects of soil water on photosynthesis were represented as follows:

$$F_{w(i)} = \begin{cases} 0 & W_{(i)} \leq W_p \\ \frac{W_{(i)} - W_p}{W_l - W_p} & W_p < W_{(i)} < W_l \\ 1 & W_l < W_{(i)} \leq W_{upper} \\ 0.5 \times (1 + \frac{W_{(i)} - 1}{W_{upper} - 1}) & W_{(i)} \geq W_{upper} \end{cases} \quad (1)$$

where $W_p$ represents the soil water content at the wilting point ($cm^3 \cdot cm^{-3}$), while $W_l$ and $W_{upper}$ denote the lower and upper limits of optimal soil water content ($cm^3 \cdot cm^{-3}$), respectively. The calculations of $W_p$, $W_l$, and $W_{upper}$ were calculated following the original Agro-C model described by Huang et al. (2009) using the site-specific soil properties as model inputs. $W_{(i)}$ is the daily mean soil water content in the 0–40 cm layer ($cm^3 \cdot cm^{-3}$). The daily soil moisture $W_{(i)}$ is calculated by balancing precipitation and actual evapotranspiration, as expressed in the following equation:

$$W_{(i)} = W_{(i)-1} + \frac{PRE_{(i)} - EA_{(i)}}{h} \quad (2)$$

$PRE_{(i)}$ and $EA_{(i)}$ represent daily precipitation (mm) and evapotranspiration (mm), respectively, while *h* denotes soil depth (mm). We assumed that precipitation is

retained within the 0–40 cm soil layer, neglecting runoff and vertical percolation. Evapotranspiration was determined jointly by the leaf area index (LAI) and potential evapotranspiration ($ET_0$) (Ritchie, 1998). $ET_0$ was calculated using the Priestley–Taylor equation (Priestley and Taylor, 1972).

In simulating vegetation photosynthesis, the Agro-C model does not account for water stress. Instead, the model determines whether irrigation is required by calculating the difference between soil water content (SWC) and the thresholds defined by the wilting point ($W_P$) and field capacity (FC) .

$$W_{diff} = W_{(i)} - ((W_{FC} - W_p) \times 0.5 + W_p) \tag{3}$$

where $W_{FC}$ represents the field capacity ($cm^3 \cdot cm^{-3}$). When $W_{diff} < 0$, the crop is considered to require irrigation. The irrigation method is defined as follows:

$$W_{(i)} = \frac{(W_{(i)} + 100)}{h} \tag{4}$$

2.3 Modelling adjustments of the water dynamics and the responsive crop photosynthate allocation

The pre-optimized Agro-C model did not explicitly account for actual irrigation inputs. To represent field irrigation practices, the optimized water module incorporates the daily irrigation amount ($W_{Irr,(i)}$) during the crop growing season as a model input. Soil moisture ($W_{(i)}$) is subsequently calculated using the recorded precipitation and irrigation data for each study site, together with the crop water supply and water demand.

$$W_{(i)} = \begin{cases} W_{(i)-1} + \dfrac{PRE_{(i)} + W_{Irr,(i)} - ET_{c,(i)}}{h} & \Delta W_{(i)} < 0 \\ W_{(i)-1} + \dfrac{PRE_{(i)} + W_{Irr,(i)} - W_{u,(i)}}{h} & \Delta W_{(i)} > 0 \end{cases} \tag{5}$$

where $\Delta W_{(i)}$ (mm) is the difference between the daily crop water requirement ($ET_c$, mm) and the actual daily water uptake ($W_{u,(i)}$, mm).

$$\Delta W_{(i)} = ET_{c,(i)} - W_{u,(i)} \tag{6}$$

When $\Delta W_{(i)} > 0$, drought stress exists; when $\Delta W_{(i)} < 0$, the crops require sufficient water.

$ET_{c,(i)}$ is calculated based on crop evapotranspiration and crop coefficient ($K_c$):

$$ET_{c,(i)} = K_c \times ET_0 \tag{7}$$

The $K_c$ values at different growth stages were derived from *FAO-56* (Allen et al., 2005).

Roots are the primary organs for water and nutrient acquisition. The root water uptake $W_{u,(i)}$ (mm) is driven by the water potential gradient between the soil and the root xylem, and regulated by the daily root hydraulic conductivity ($C_{r,(i)}$, $MPa^{-1}$) of that layer (Hafner et al., 2020).

$$W_{u,(i)} = \Delta\psi_{(i)} \times C_{r,(i)} \tag{8}$$

The root-soil water potential difference $\Delta\psi_{(i)}$ is primarily determined by the soil water potential $\psi_{s,(i)}$ (MPa), as root water potential $\psi_{r,(i)}$ (MPa) within a relatively stable range through osmoregulation (Dodd et al., 2010). The $\psi_{r,(i)}$ can be treated as an empirical constant derived from literature (Munns and Tester, 2008; Novák et al., 2005). The $\psi_{s,(i)}$ can be calculated using the van Genuchten water retention function (van Genuchten, 1980).

$$\psi_{s,(i)} = \frac{1}{\alpha}\left[\left(\frac{\theta_s - \theta_r}{W_{(i)} - \theta_r}\right)^{1/m} - 1\right]^{1/n}, \quad m = 1 - \frac{1}{n} \tag{9}$$

where $\theta_s$ denotes the saturated soil moisture content ($cm^3\ cm^{-3}$), $\theta_r$ denotes the residual soil moisture content ($cm^3\ cm^{-3}$). The $\alpha$ and $n$ represent the empirical parameters of van Genuchten related to soil texture. These parameters were derived according to the parameterization scheme of the original Agro-C model (Huang et al., 2009).

$$\Delta\psi_i = (\psi_{s,(i)} - \psi_{r,(i)}) \tag{10}$$

The root hydraulic conductivity ($C_{r,(i)}$) represents the water flux from a unit volume of soil per unit water potential gradient. It is calculated as the product of the

total root surface area in that soil volume and the intrinsic hydraulic conductance per unit root surface area ($Lp_r$, $m \cdot d^{-1} \cdot Mpa^{-1}$).

$$C_{r,(i)} = (M_{r,(i)-1} \times S_r) \times Lp_r \tag{11}$$

where $M_{r,(i)-1}$ is the root dry mass per unit soil volume ($g \cdot m^{-3}$), $S_r$ is the specific root surface area ($m^2 \cdot g^{-1}$). To avoid circular dependency and ensure numerical stability, $W_{u,(i)}$ was calculated using root biomass from the previous time step. The term ($M_{r,(i)-1} \times S_r$) thus gives the root surface area density. Values of $Lp_r$ for maize (Steudle, 2000; Cai et al., 2022; Rishmawi et al., 2023; Protto et al., 2024) and wheat ( Cai et al., 2022; Yang et al., 2023) at different developmental stages were obtained from the literature.

## 2.4 Calibration of photosynthate allocation coefficients in the Agro-C model

In the Agro-C model, the crop development index (DVI) is defined as 0 at emergence, 1 at heading for wheat or silking for maize, and 2 at maturity. The DVI is divided into 21 intervals at increments of 0.1. Within each interval, the proportion of assimilates allocated to leaves (PL) and roots (PR) is fixed (Huang et al., 2009), while the proportion allocated to stems is calculated as 1 – (PL + PR). During the vegetative growth stage, the allocation of dry matter to roots and leaves decreases with development, whereas during the reproductive stage, all assimilates are allocated exclusively to grains (Table S1).

Jiang et al. (2018) demonstrated that under water stress, the photosynthate allocation ratios to roots, stems, and leaves all vary with water availability. Therefore, in the Agro-C model, the pre-optimized allocation ratios for leaves and roots need to be appropriately adjusted ($\Delta PL_{(i)}$ and $\Delta PR_{(i)}$) to enable the model to capture assimilate allocation mechanisms under different water conditions. The calibrated allocation coefficients for leaves and roots ($PL_{N(i)}$ and $PR_{N(i)}$) are thus obtained by adding the adjustment terms to the pre-optimized coefficients ($PL_{O(i)}$ and $PR_{O(i)}$).

$$PL_{N(i)} = PL_{O(i)} + \Delta PL_{(i)} \tag{12}$$

$$PR_{N(i)} = PR_{O(i)} + \Delta PR_{(i)} \tag{13}$$

In the initial stage of model calibration, before clarifying the relationships of $\Delta PL_{(i)}$ and $\Delta PR_{(i)}$ with water availability, constant values of $\Delta PL_{(i)}$ and $\Delta PR_{(i)}$ were preliminarily assigned. The feasibility of these values was then evaluated by comparing the simulated aboveground and belowground biomass (Sim_AGB, Sim_BGB) with the observed values (Obs_AGB, Obs_BGB). If both ratios Sim_AGB / Obs_AGB and Sim_BGB / Obs_BGB exceeded 80%, the assigned $\Delta PL_{(i)}$ and $\Delta PR_{(i)}$ were considered acceptable (Fig. 1).

After the initial calibration of the model, correlation equations between $\Delta PL_{(i)}$, $\Delta PR_{(i)}$, and $\Delta W_{(i)}$ were developed. These equations were then used to replace the initially assigned constant values, thereby providing a more accurate and explicit representation of the changes in photosynthate allocation coefficients under soil water stress.

Drought stress accelerates leaf senescence, abscission, and mortality, thereby altering the yellow-to-green leaf ratio (YGR) (Seleiman et al., 2021). In addition to calibrating the photosynthate allocation coefficients, we also adjusted the $YG_R$ parameter in the pre-optimized Agro-C model. Specifically, correlation equations between the increment of the yellow-to-green leaf ratio ($\Delta YGR_{(i)}$) and $\Delta W_{(i)}$ were developed to represent the calibrated YGR ($YGR_{N(i)}$) under dynamically varying soil water conditions.

$$YGR_{N(i)} = YGR_{O(i)} + \Delta YGR_{(i)} \tag{14}$$

where $YGR_{O(i)}$ represents the yellow-to-green leaf ratio in the pre-optimized Agro-C model.

To simplify the model, we further incorporated the DVI as an additional independent variable in the above equations, thereby accounting for the combined effects of water availability and crop developmental stage on photosynthate allocation.

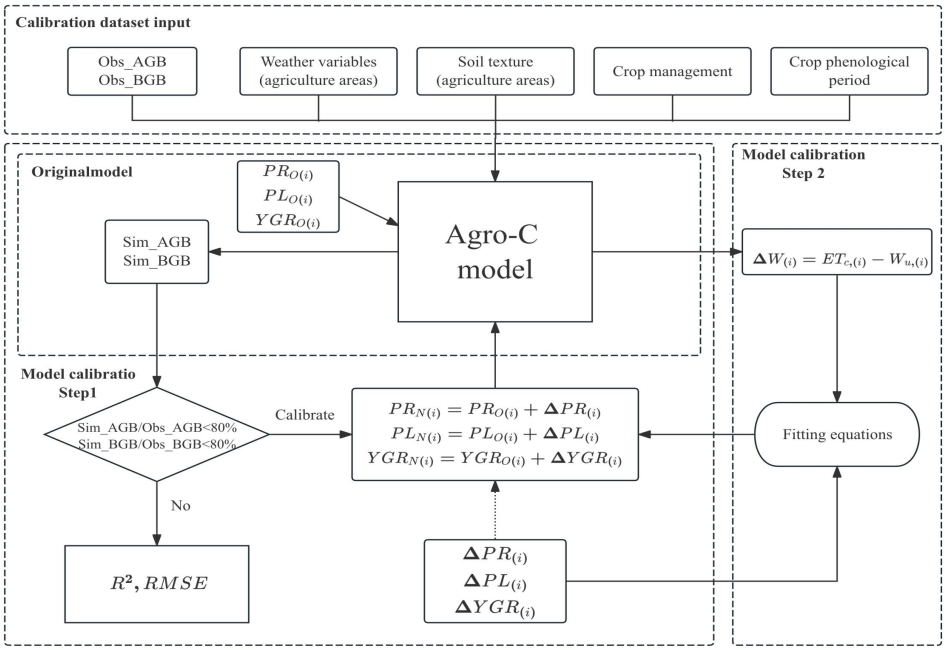


Fig. 1 Flowchart of Agro-C model parameter optimization

## 2.5 Data input and model evaluation

The input variables included: meteorological data (solar radiation, sunshine duration, daily maximum and minimum temperature, and precipitation); soil data (bulk density, sand and clay content, and total nitrogen content); phenological data (for wheat: emergence, heading, and maturity; for maize: emergence, tasseling, and maturity); and management practices (irrigation amount, fertilizer N application rate, and timing of application).

If irrigation amounts ($W_{irr,(i)}$) were recorded at the experimental sites for each crop growth stage, the values were directly input according to the recorded dates. If no specific irrigation amounts were available but the relative available soil water (RAW) during the growing season was recorded, the given RAW was used as the upper threshold ($W_t$) to estimate irrigation. Irrigation was triggered when the model-simulated RAW dropped 10% below the site-defined threshold. The soil relative water content used in the model was calculated as follows:

$$\mathrm{RAW} = \frac{W_{(i)} - W_P}{W_{FC} - W_P} \times 100\% \tag{15}$$

where $W_{(i)}$ is the actual soil water content (v/v), $W_P$ is the crop wilting point (v/v), and

$W_{FC}$ is the field capacity of the soil (v/v).

Irrigation amount was calculated as follows (Ge et al., 2012):

$$W_{irr,(i)} = (W_t - W_{(i)}) \times \rho \times h \times 0.1 \quad (16)$$

where $W_t$ is the target upper limit of soil water content (v/v), $\rho$ is the soil bulk density (g $cm^{-3}$), and $h$ is the thickness of the soil layer considered (cm).

We used the coefficient of determination ($R^2$) and the root mean squared error (RMSE) as evaluation metrics to assess prediction accuracy, which are defined as follows:

$$R^2 = \frac{\sum_i (y_i - \widehat{y_i})^2}{\sum_i (y_{ii} - \overline{y})^2} \quad (17)$$

$$RMSE = \sqrt{\frac{\sum_{i=1}^{n} (y_i - \widehat{y_i})^2}{n}} \quad (18)$$

where n is the number of test samples, $y_i$ is the $i$ observed value, $\bar{y}$ is the mean of all observed values, $\widehat{y_i}$ is the $i$ simulated value.

## 3. Results

### 3.1 Optimization equations for photosynthate coefficients in response to soil moisture variation

#### *3.1.1 Parameter optimization equations*

To facilitate computation and maintain a balance between physiological resolution and numerical stability, the DVI was divided into 0.2 intervals, each representing a distinct growth stage relevant to crop development. To better capture the intra-stage variation of allocation coefficients, DVI itself was also included as an independent variable in the equations (Tables 1 and 2). The equations in Tables 1 and 2 are empirical parameterization functions describing the responses of ΔPR, ΔPL, and ΔYGR to water deficit (ΔW) at different DVI stages. The appropriate equation should be selected according to the crop type, DVI interval, and ΔW value during model

simulation.

Consistent with the pre-optimized allocation scheme of the model, we assumed that no leaf senescence occurred during the early vegetative stage (DVI < 0.6 for maize, DVI < 0.8 for wheat), with $YG_{R_N} = 0$; and during the late reproductive stage (DVI > 1.4), assimilates were allocated only to grains, with the leaf allocation coefficient set to zero. In the pre-optimized Agro-C model, assimilate allocation to roots ($PR_N$) was also assumed to cease once the crop entered the reproductive stage under sufficient water supply. However, our previous study (Xu et al., 2025) indicated that under water stress, assimilates may continue to be allocated to roots during the reproductive phase to facilitate water uptake and sustain growth. In addition, during the grain-filling to maturity stages (DVI=1.4–2.0), crops gradually enter physiological senescence, and fine roots undergo necrosis and shedding, leading to reduced root dry matter accumulation. Therefore, we further refined the root allocation scheme during the reproductive stage, building upon the pre-optimized framework.

Table 1 Wheat increments of Root (ΔPR) and Leaf (ΔPL) Allocation Coefficients, Yellow-to-Green Leaf Ratio (ΔYGR), and Water Balance Difference ($\Delta W_{(i)}$) Equation

$$a + b \times \Delta W_{(i)} + c \times DVI + d \times \Delta W_{(i)}^2 + e \times \Delta W_{(i)} \times DVI + f \times DVI^2$$

| DVI | | a | b | c | d | e | f | $R^2$ | n | Range |
|---|---|---|---|---|---|---|---|---|---|---|
| (0.0, 0.2] | ΔPR | 0.16 | -0.29 | -0.51 | -0.13 | 1.47 | 1.40 | 0.06 | 438 | [-0.1, 0.05] |
| | ΔPL | -0.56 | 3.32 | 6.83 | 1.72 | -19.62 | -17.95 | 0.13 | | [0.05, 0.15] |
| | ΔYGR | | | | 0.00 | | | | | |
| (0.2, 0.4] | ΔPR | 0.98 | -0.62 | -4.80 | 0.27 | 1.76 | 5.24 | 0.57 | 2150 | [-0.2, 0.1] |
| | ΔPL | -8.73 | -2.84 | 50.93 | 0.81 | 8.29 | -72.50 | 0.20 | | [-0.1, 0.29] |
| | ΔYGR | | | | 0.00 | | | | | |
| (0.4, 0.6] | ΔPR | 0.20 | 0.12 | -1.92 | -0.02 | -0.17 | 2.24 | 0.18 | 2567 | [-0.26, 0.1] |
| | ΔPL | -1.99 | -1.43 | 7.92 | 0.01 | 2.32 | -7.10 | 0.10 | | [-0.16, 0.39] |
| | ΔYGR | | | | 0.00 | | | | | |
| (0.6, 0.8] | ΔPR | 0.21 | -0.11 | -1.16 | 0.02 | 0.10 | 1.08 | 0.47 | 655 | [-0.1, 0.0] |
| | ΔPL | -2.35 | -0.51 | 9.15 | 0.14 | 0.71 | -8.33 | 0.16 | | [-0.15, 0.35] |
| | ΔYGR | | | | 0.00 | | | | | |
| (0.8, 1.0] | ΔPR | -0.03 | 0.01 | -0.49 | 0.00 | -0.01 | 0.58 | 0.49 | 439 | [-0.12, 0.15] |
| | ΔPL | -5.28 | 0.37 | 11.31 | 0.05 | -0.64 | -5.64 | 0.07 | | [-0.17, 0.46] |
| | ΔYGR | -0.57 | -0.28 | 0.84 | 0.01 | 0.32 | -0.72 | 0.05 | | [-0.43, 0.25] |
| (1.0, 1.2] | ΔPR | 3.98 | 0.79 | -7.82 | 0.00 | -0.66 | 3.77 | 0.24 | 388 | [-0.06, 0.06] |
| | ΔPL | -27.75 | -1.10 | 54.01 | 0.07 | 0.95 | -26.12 | 0.14 | | [0.0,0.36] |
| | ΔYGR | -21.40 | -0.95 | 45.10 | -0.06 | 0.92 | -23.86 | 0.52 | | [-1.8, 0.4] |
| (1.2, 1.4] | ΔPR | -4.72 | -0.01 | 7.46 | -0.04 | 0.06 | -2.97 | 0.14 | 305 | [-0.1, 0.05] |
| | ΔPL | 1.40 | 0.42 | -1.82 | -0.01 | -0.30 | 0.59 | 0.17 | | [0.0, 0.2] |
| | ΔYGR | -8.49 | 6.08 | 12.73 | -0.06 | -4.76 | -6.02 | 0.35 | | [-3.85, 0.68] |
| (1.4, 1.6] | ΔPR | -21.91 | -1.31 | 28.98 | -0.02 | 0.86 | -9.60 | 0.12 | 304 | [-0.06, 0.0] |
| | ΔPL | | | | 0.00 | | | | | |
| | ΔYGR | -273.12 | -5.71 | 379.64 | -0.21 | 4.35 | -133.41 | 0.14 | | [-5.0, 0.0] |
| (1.6, 1.8] | ΔPR | 30.50 | 1.87 | -38.69 | 0.00 | -1.14 | 12.22 | 0.09 | 288 | [-0.06, -0.03] |
| | ΔPL | | | | 0.00 | | | | | |
| | ΔYGR | -510.13 | 1.23 | 612.27 | 0.69 | -1.96 | -184.75 | 0.11 | | [-6.4, 0.0] |
| (1.8, 2] | ΔPR | 9.68 | -9.64 | -9.06 | -0.26 | 5.31 | 2.04 | 0.16 | 268 | [-0.06, 0.0] |
| | ΔPL | | | | 0.00 | | | | | |
| | ΔYGR | -551.31 | 285.62 | 548.12 | 8.42 | -157.41 | -136.47 | 0.18 | | [-7.5, 0.0] |

Table 2 Maize increments of Root (ΔPR) and Leaf (ΔPL) Allocation Coefficients, Yellow-to-Green Leaf Ratio (ΔYGR), and Water Balance Difference ($\Delta W_{(i)}$) Equation

$a + b \times \Delta W_{(i)} + c \times DVI + d \times \Delta W_{(i)}^2 + e \times \Delta W_{(i)} \times DVI + f \times DVI^2$

| DVI | | a | b | c | d | e | f | $R^2$ | n | Range |
|---|---|---|---|---|---|---|---|---|---|---|
| (0.0, 0.2] | ΔPR | -0.15 | -0.70 | -0.09 | 0.53 | 3.76 | -1.05 | 0.98 | 435 | [-0.2, -0.1] |
| | ΔPL | 0.19 | 0.56 | 0.07 | -0.42 | 3.01 | 0.84 | 0.89 | | [0.19, 0.23] |
| | ΔYGR | | | | 0.00 | | | | | |
| (0.2, 0.4] | ΔPR | 0.60 | -1.09 | -6.22 | 0.34 | 3.84 | 11.35 | 0.89 | 383 | [-0.25, -0.2] |
| | ΔPL | -3.09 | 4.20 | 24.02 | -1.22 | -14.89 | -43.57 | 0.90 | | [0.05, 0.22] |
| | ΔYGR | | | | 0.00 | | | | | |
| (0.4, 0.6] | ΔPR | 5.47 | -0.67 | -26.86 | 0.00 | 1.52 | 31.64 | 0.92 | 389 | [-0.25, 0.0] |
| | ΔPL | 1.47 | 0.12 | -5.41 | 0.07 | -0.42 | 4.32 | 0.76 | | [0.0, 0.22] |
| | ΔYGR | | | | 0.00 | | | | | |
| (0.6, 0.8] | ΔPR | -0.89 | 0.80 | 2.22 | 0.02 | -1.11 | -1.38 | 0.23 | 348 | [-0.05, 0.05] |
| | ΔPL | -1.51 | -0.09 | 3.44 | 0.00 | 0.13 | -2.27 | 0.62 | | [-0.1, 0.11] |
| | ΔYGR | 2.26 | -2.84 | -5.48 | -0.09 | 3.97 | 3.36 | 0.24 | | [-0.03, 0.2] |
| (0.8, 1.0] | ΔPR | | | | 0.00 | | | | 332 | |
| | ΔPL | 29.56 | -0.43 | -69.90 | 0.00 | 0.48 | 41.16 | 0.88 | | [-0.2, 0.11] |
| | ΔYGR | -65.17 | 0.40 | 151.25 | 0.00 | -0.10 | -87.51 | 0.43 | | [-0.07, 0.35] |
| (1.0, 1.2] | ΔPR | -6.08 | 1.11 | 9.59 | -0.01 | -1.01 | -3.62 | 0.66 | 308 | [0.0, 0.12] |
| | ΔPL | -118.10 | 2.26 | 206.59 | 0.07 | -1.74 | -90.19 | 0.42 | | [0.05, 0.45] |
| | ΔYGR | 12.14 | -0.05 | -19.86 | -0.05 | 0.03 | 7.99 | 0.42 | | [-0.14, 0.3] |
| (1.2, 1.4] | ΔPR | 117.85 | -1.74 | -172.01 | 0.04 | 1.18 | 62.85 | 0.38 | 321 | [0.0, 0.12] |
| | ΔPL | -213.00 | 3.34 | 311.30 | -0.07 | -2.28 | -113.67 | 0.37 | | [0.0, 0.4] |
| | ΔYGR | 120.52 | -2.50 | -175.84 | 0.05 | 1.72 | 64.04 | 0.40 | | [-0.48, 0.17] |
| (1.4, 1.6] | ΔPR | 174.42 | 9.21 | -247.65 | 0.13 | -6.55 | 87.92 | 0.54 | 338 | [-0.05, 0.12] |
| | ΔPL | | | | 0.00 | | | | | |
| | ΔYGR | 229.20 | 11.38 | -326.10 | 0.16 | -8.11 | 115.83 | 0.53 | | [-0.5, 0.0] |
| (1.6, 1.8] | ΔPR | 259.85 | 3.67 | -295.73 | -0.03 | -1.96 | 84.05 | 0.31 | 370 | [-0.15, 0.0] |
| | ΔPL | | | | 0.00 | | | | | |
| | ΔYGR | -838.08 | 6.24 | 1010.12 | 0.12 | -4.20 | -304.31 | 0.62 | | [-0.3, 0.15] |
| (1.8, 2] | ΔPR | 0.80 | 3.13 | -1.45 | -0.20 | -1.60 | 0.53 | 0.34 | 439 | [-0.15, 0.0] |
| | ΔPL | | | | 0.00 | | | | | |
| | ΔYGR | -246.13 | 16.95 | 263.13 | 0.90 | -9.58 | -70.43 | 0.38 | | [-0.6, 0.3] |

### *3.1.2 Response of photosynthate allocation coefficients to soil moisture changes*

We further analyzed the variation in assimilate allocation coefficients (PR , PL, and YGR) in response to soil moisture levels during key growth stages, including the jointing stage, silking stage (maize), heading stage (wheat), and maturity (Fig. 2).

At the jointing stage (DVI = 0.4–0.6), maize PL significantly decreased with increasing soil moisture, while PR also showed a slight downward trend (Fig. 2(a)). In contrast, wheat PL was relatively insensitive to moisture changes, but under severe drought stress condition (RAW < 45%), wheat PR was significantly lower than under well-watered conditions (Fig. 2(d)). During the silking stage of maize (DVI = 1.0–1.2), both PL and YGR decreased with increasing soil moisture under moderate drought stress condition (RAW = 45–60%) and severe drought stress. However, under mild drought (RAW = 60–70%) to optimal moisture conditions, both PL and YGR increased with rising soil moisture. The PR exhibited a non-linear response, increasing first and then decreasing as moisture increased (Fig. 2(b)). Similarly, at the wheat heading stage (DVI = 1.0–1.2), the trend of PR and YGR was comparable to that of maize, whereas wheat PL continuously decreased with increasing soil moisture, which is in contrast to maize (Fig. 2(e)).

At the maturity stage (DVI = 1.8–2.0), photosynthates were no longer allocated to leaves but instead to grains. Under drought stress, maize YGR increased significantly (Fig. 2(c)). Moreover, excessive soil moisture condition (RAW > 85%) also led to higher YGR values than under optimal condition (RAW = 70–85%). The PR increased with rising soil moisture during this stage, as extreme drought caused premature root senescence and decay. Conversely, wheat PR and YGR decreased with increasing soil moisture during maturity (Fig. 2(f)). Notably, under severe drought conditions, wheat YGR was lower than under other moisture levels.

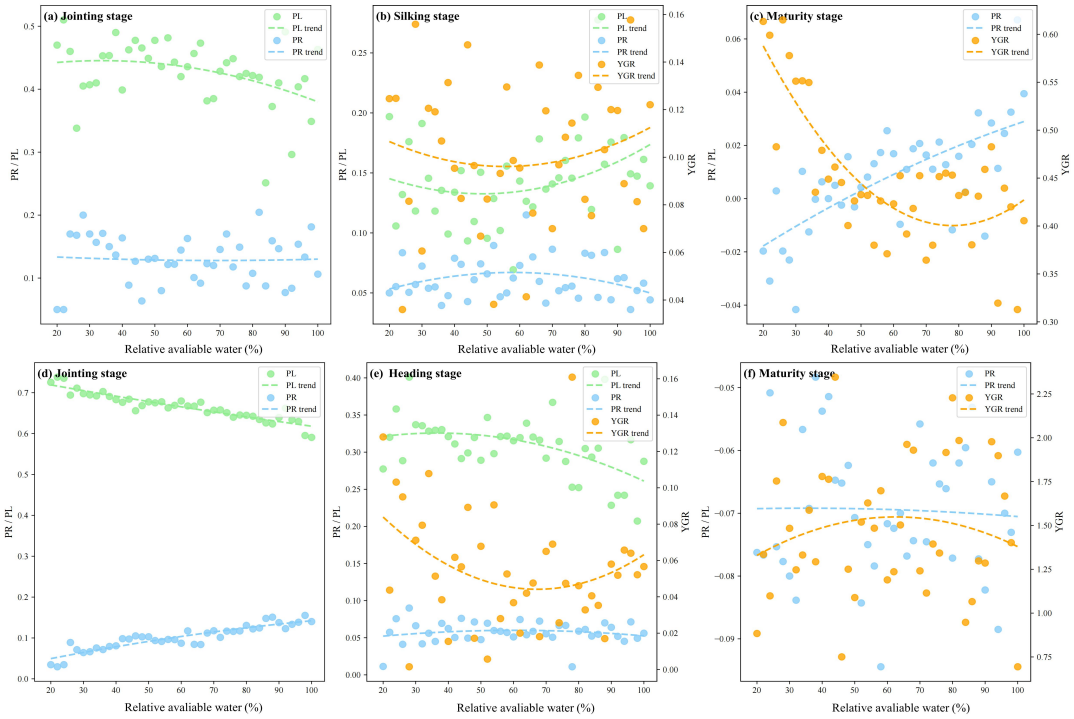


Fig. 2 Mean values and fitted curves of the leaf allocation coefficient (PL), root allocation coefficient (PR), and yellow-to-green leaf ratio (YGR) for maize and wheat at the jointing, silking/heading, and maturity stages under different soil moisture conditions, as simulated by the optimized Agro-C model. PL and PR share the left y-axis, whereas YGR is plotted on the right y-axis.

## 3.2 Model calibration and validation

### *3.2.1 Calibration results*

We selected datasets that provided detailed records of AGB and BGB at multiple crop growth stages, and which included experimental treatments under different levels of water stress, to serve as the calibration dataset. This allowed for more accurate simulation of photosynthate allocation across developmental stages.

Overall, the optimized Agro-C model showed higher accuracy in simulating AGB, with $R^2$ values exceeding 0.56 across all growth stages. In contrast, the simulation accuracy for BGB was relatively lower, with $R^2$ values ranging from 0.33 to 0.72 (Fig. 3). Notably, the optimized Agro-C model performed well in simulating AGB at maturity (Fig. 3(c)), with $R^2$ values of 0.89 for maize and 0.68 for wheat. Improved accuracy in simulating AGB at maturity contributes to more reliable estimation of crop productivity. The optimized Agro-C model showed better

performance in simulating wheat BGB ($R^2$ = 0.72) at the jointing stage compared to maize ($R^2$ = 0.65). However, during the reproductive stage (silking to maturity for maize; heading to maturity for wheat), simulation accuracy was higher for maize. For maize, the optimized Agro-C model consistently achieved $R^2$ values above 0.63 across all growth stages, indicating a good performance.

Although the optimized Agro-C model showed relatively low $R^2$ values for simulating wheat BGB at heading and maturity stages (0.33 and 0.44, respectively; Fig. 3(e-f)), this was primarily attributed to physiological root senescence during late reproductive stages, leading to lower root biomass per unit area. Under such conditions, the absolute values of BGB were small, and even slight deviations between simulated and observed values could substantially reduce $R^2$. Nevertheless, the RMSE for wheat BGB at heading and maturity were 8.45 and 8.23 gC $m^{-2}$, respectively, indicating relatively small deviations. Therefore, we consider the optimized Agro-C model to be reasonably reliable and practically applicable for simulating BGB for wheat during the later reproductive stages.

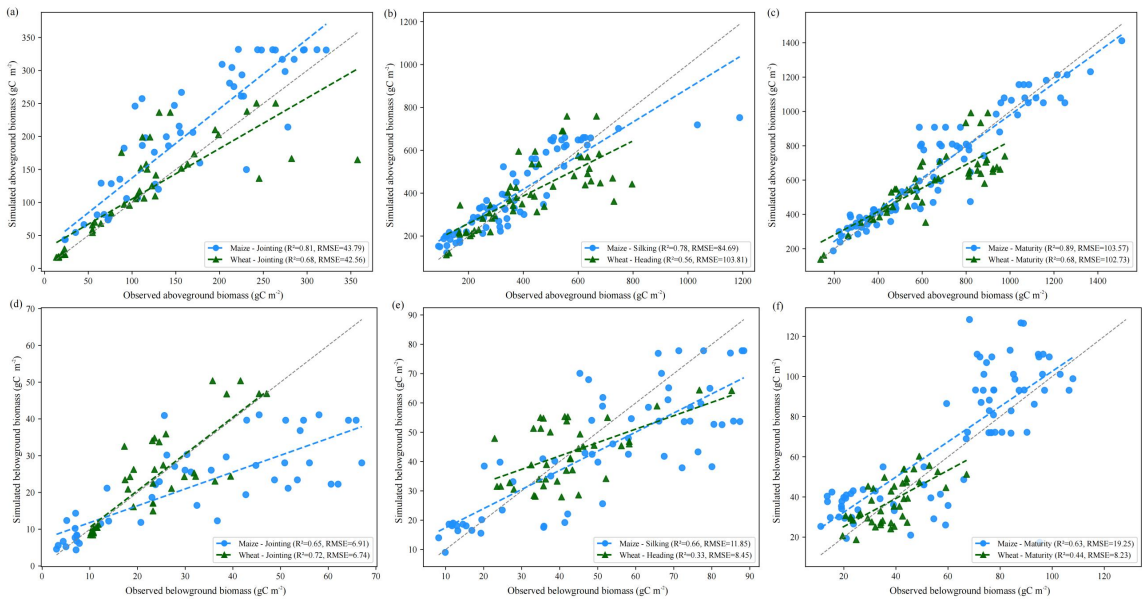


Fig. 3 Calibration results of the Agro-C model for aboveground biomass (AGB) and belowground biomass (BGB) of maize and wheat at the jointing, heading/grain-filling, and maturity stages. (a)-(c) show AGB calibration results; (d)-(f) show BGB calibration results. Blue circles represent maize, and green triangles represent wheat.

### *3.2.2 Validation results*

Due to limited availability of experimental data, the criteria for selecting the validation dataset were less stringent than those applied to the calibration dataset. Therefore, datasets that included detailed records of water use during the crop growth period (regardless of whether water stress treatments were applied) and biomass data for one or more growth stages were included in the validation dataset.

Compared with the pre-optimized Agro-C model, the optimized Agro-C model showed substantial improvements in simulating assimilate production for both maize and wheat (Fig. 4). For maize, the simulation accuracy for AGB improved from $R^2$ = 0.70 and RMSE = 153.15 gC $m^{-2}$ to $R^2$ = 0.95 and RMSE = 66.03 gC $m^{-2}$. Similarly, the BGB simulation improved from $R^2$ = 0.49 and RMSE = 20.55 gC $m^{-2}$ to $R^2$ = 0.61 and RMSE = 11.18 gC $m^{-2}$. Likewise, for wheat, the optimized Agro-C model significantly improved the simulation accuracy for both AGB and BGB, achieving $R^2$ values of 0.74 (RMSE = 60.26 gC $m^{-2}$) for AGB and 0.48 (RMSE = 19.43 gC $m^{-2}$) for BGB, compared to the pre-optimized Agro-C model, which simulated AGB and BGB much lower $R^2$ values of 0.31 and 0.42, respectively. The validation dataset comprised several water-stress treatments, and the pre-optimized Agro-C model simulation accuracy declined under these conditions due to the absence of water stress-responsive allocation parameters in the pre-optimized structure.

Similar to the calibration results, the optimized Agro-C model exhibited significantly higher accuracy in simulating AGB than BGB for the validation dataset. However, after parameter optimization, the average differences between simulated and observed BGB for maize and wheat were only 5.19 and -2.52 gC $m^{-2}$, respectively (Fig. S2), indicating relatively small deviations. In addition, compared to the pre-optimized Agro-C model, the optimized Agro-C model exhibited consistently smaller deviations from the observed values (Fig. S2), suggesting a relatively reliable parameter calibration scheme.

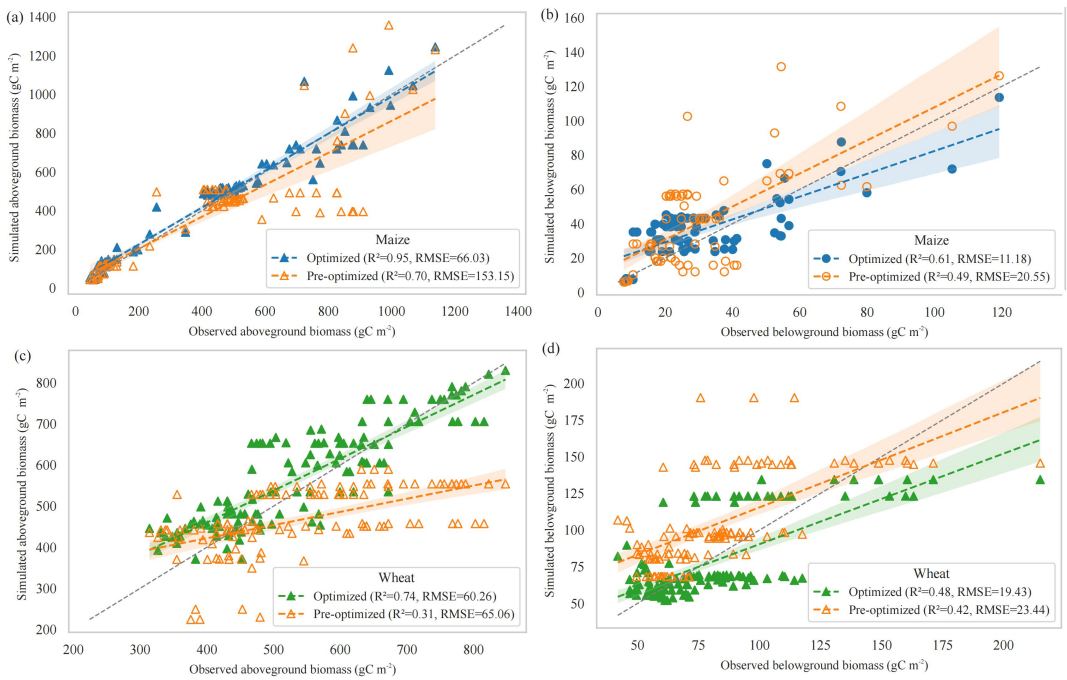


Fig. 4 Validation results of the pre-optimized and optimized Agro-C model for simulating aboveground biomass (AGB) and belowground biomass (BGB) of maize and wheat. (a) and (b) show the validation results for maize AGB and BGB, respectively; (c) and (d) show the validation results for wheat AGB and BGB, respectively. Blue circles and green triangles represent the simulation results from the optimized model, while orange hollow circles and triangles represent the simulation results from the pre-optimized Agro-C model for maize and wheat, respectively.

### 3.3 Simulating photosynthate under different RAW

Based on the observed patterns, four distinct soil moisture regimes were defined: severe drought (RAW < 45%), mild-to-moderate drought (RAW = 45–70%), optimal moisture (RAW = 70–85%), and excessive moisture (RAW > 85%). Simulations of maize and wheat AGB and BGB were conducted under each condition (Figs. 5-8).

Since the pre-optimized Agro-C model did not adequately account for crop growth under water-deficit conditions, its performance in simulating photosynthate production under water stress (RAW < 70%) was unsatisfactory, resulting in low $R^2$ values and relatively high RMSE. However, under optimal moisture conditions, the pre-optimized model performed well, particularly in simulating AGB, demonstrating its high applicability in well-watered environments. The optimized Agro-C model showed marked improvements across all moisture regimes. The $R^2$ of AGB simulation for maize ranged from 0.77 to 0.95, and for wheat from 0.80 to 0.89,

respectively (Figs. 5 and 7), demonstrating that the optimized Agro-C model performed well in simulating AGB across different soil moisture conditions. This strong performance enhances its applicability for crop productivity estimation and quantification of straw return to the field. For wheat BGB, the optimized Agro-C model achieved $R^2$ values of 0.77–0.83 (Fig. 8), greatly improving the accuracy compared to the pre-optimized Agro-C model ($R^2$ in 0.52–0.78), which previously exhibited large errors in simulating wheat BGB. Under varying soil moisture conditions, the optimized Agro-C model achieved $R^2$ values of 0.62 to 0.74 for simulating maize BGB, consistently outperforming pre-optimized Agro-C model. Notably, the accuracy of the optimized Agro-C model was significantly improved under severe and mild-to-moderate drought, highlighting its enhanced responsiveness to water stress.

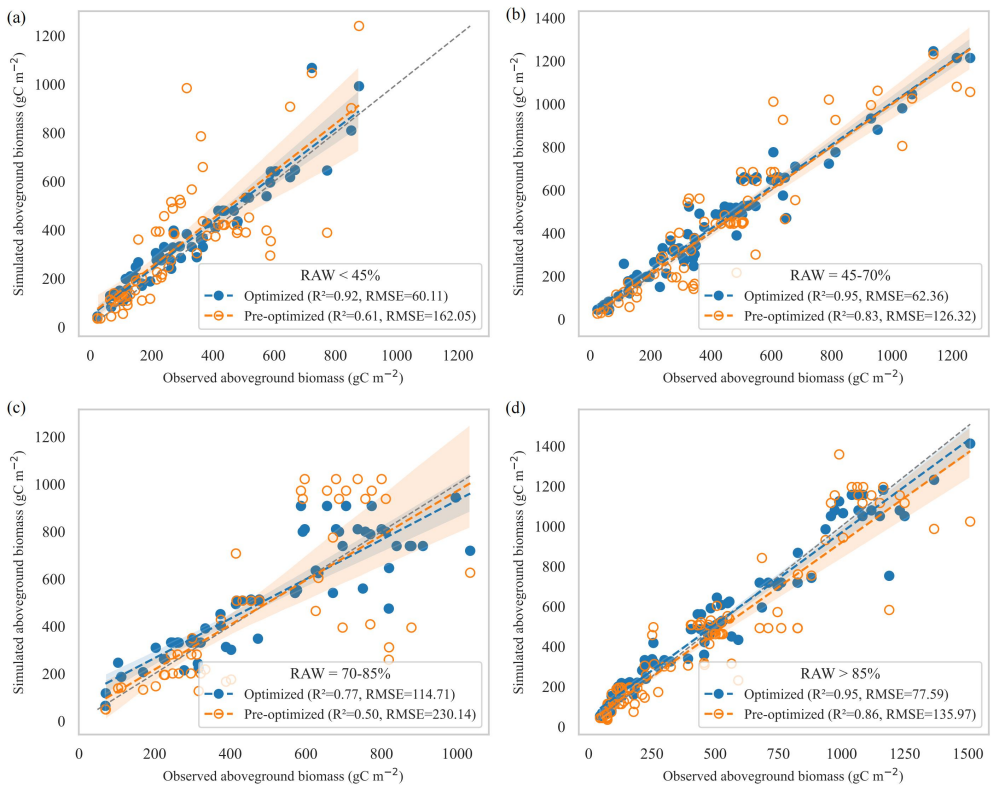


Fig. 5 Simulated aboveground biomass (AGB) of maize under different relative available soil water (RAW) conditions using the pre-optimized Agro-C model and the optimized Agro-C model. Blue circles represent simulation results from the optimized Agro-C model, and orange circles represent those from the pre-optimized Agro-C model.

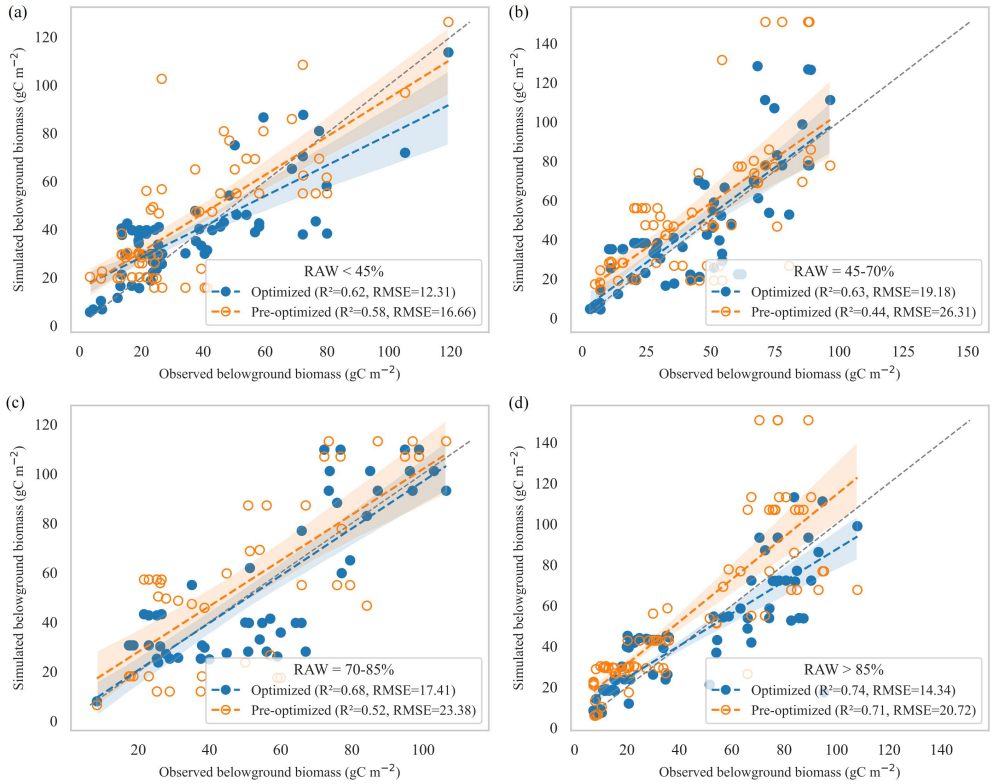


Fig. 6 Simulated belowground biomass (BGB) of maize under different relative available soil water (RAW) conditions using the pre-optimized Agro-C model and the optimized Agro-C model. Blue circles represent simulation results from the optimized Agro-C model, and orange circles represent those from the pre-optimized Agro-C model.

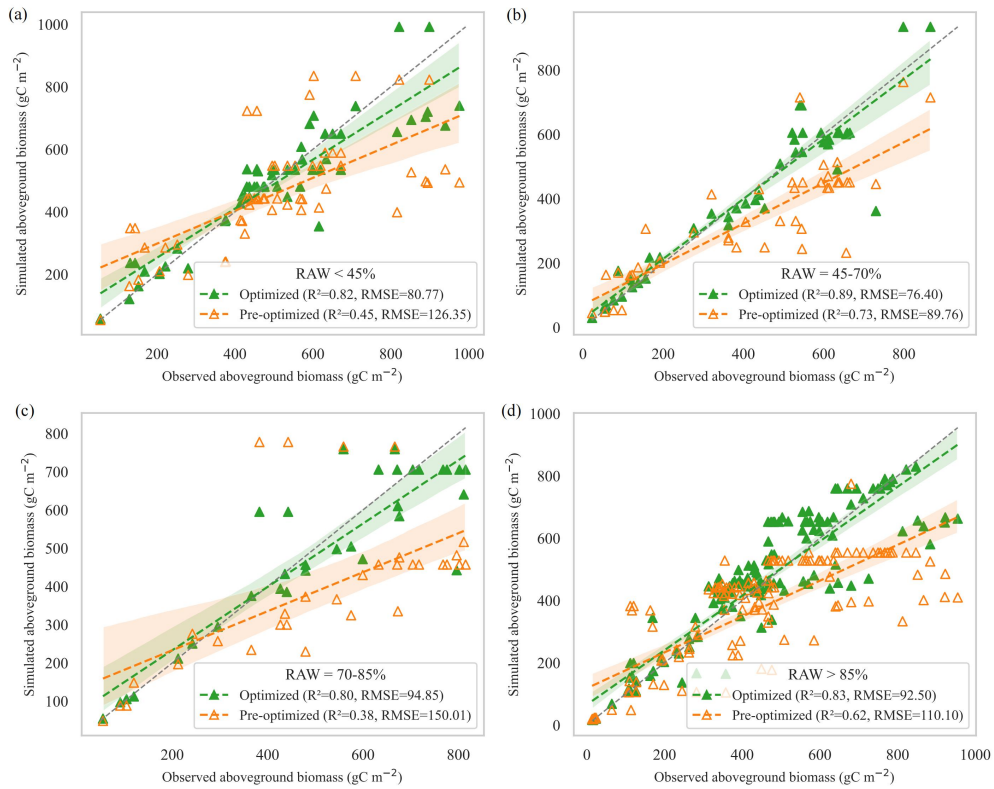

Fig. 7 Simulated aboveground biomass (AGB) of wheat under different relative available soil water (RAW) conditions using the pre-optimized Agro-C model and the optimized Agro-C model. Green triangles represent simulation results from the optimized Agro-C model, and orange triangles represent those from the pre-optimized Agro-C model.

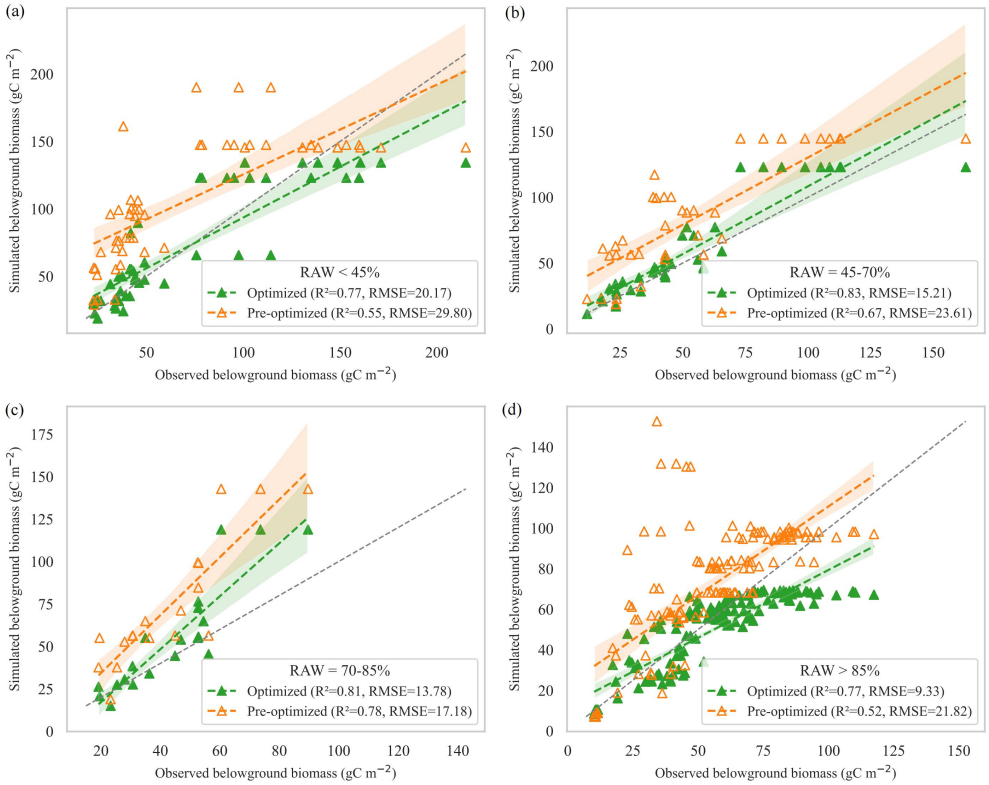


Fig. 8 Simulated belowground biomass (BGB) of wheat under different relative available soil water (RAW) conditions using the pre-optimized Agro-C model and the optimized Agro-C model. Green triangles represent simulation results from the optimized Agro-C model, and orange triangles represent those from the pre-optimized Agro-C model.

## 4. Discussion

### 4.1 Model performance evaluation

By incorporating dynamic response functions of photosynthate allocation to water stress and crop development, the optimized Agro-C model substantially improved the simulation of crop growth across all developmental stages in both maize and wheat. Overall, the model exhibited higher accuracy for simulating AGB than BGB, a trend consistently observed in both the calibration and validation datasets (Figs. 3 and 4). This difference likely reflects the greater availability of observational data and the more comprehensive understanding of aboveground physiological

processes, which together contribute to more reliable model parameterization and improved predictive performance (Asseng et al., 2013; Li et al., 2015).

Although the optimized Agro-C model better simulated wheat AGB and BGB during the jointing stage, its accuracy was surpassed by maize simulations during the reproductive phase. This contrast can be attributed to the distinct allocation strategies between the two crops during the reproductive transition. For wheat, photosynthate allocation during the jointing stage characterized primarily by leaf expansion and root development, which are relatively well represented in crop models. However, during the reproductive phase, grain filling in wheat relies heavily on the remobilization of stem-reserved assimilates (Bertheloot et al., 2008; Effah et al., 2022), while the root system undergoes rapid senescence (Wang et al., 2014), complicating model representation.

The simplified model structure does not fully represent the complexity of belowground processes, resulting in relatively low $R^2$ values (0.33–0.44) during the heading and maturity stages. Nevertheless, due to small BGB magnitudes, even modest deviations result in relatively low RMSE values (8.45 and 8.23 gC $m^{-2}$), indicating reasonable model performance at the magnitude level. In contrast, as a C4 crop, maize relies more directly on continuous leaf photosynthesis for grain formation (Boyer & Westgate, 2004). Water stress significantly suppresses leaf expansion and photosynthetic activity, but leaf area index can recover following rehydration, enhancing aboveground dry matter accumulation (Ma et al., 2025). Therefore, the dynamic adjustment of water and leaf allocation functions enhances model performance for simulating maize biomass during the reproductive stage.

Because of multiple water stress treatments in the validation dataset, the pre-optimized Agro-C model exhibited relatively limited performance (low $R^2$ and high RMSE), likely due to its inability to explicitly represent crop responses to water stress. In contrast, the optimized Agro-C model more accurately captured photosynthate allocation under water stress (Figs. 4 and S2). This further demonstrates that incorporating water-sensitive parameters into allocation functions is

a critical strategy for enhancing the drought responsiveness of crop models (Monteleone et al., 2023; Hammer et al., 2010). After parameter optimization, the simulation accuracy of Agro-C was significantly improved across all water regimes, especially for the belowground biomass simulation. Agro-C is a coupled Crop-C and Soil-C model (Huang et al., 2009), in which simulated crop residues and root biomass are directly transferred to the Soil-C module as carbon inputs. Therefore, improving photosynthate allocation reduces uncertainties in residue and root carbon inputs, especially belowground carbon, providing a more reliable basis for SOC simulation.

### 4.2 Effect of soil water on photosynthate allocation across crop growth

The response of photosynthate allocation to water stress exhibits strong stage dependence and crop specificity. The continuous DVI-based allocation functions (Tables 1 and 2) showed that drought stress altered photosynthate allocation during the vegetative stage in both maize and wheat. Specifically, carbon allocation shifted from leaves to roots, as evidenced by increased PR and decreased PL (Fig. 2(a) and (d)), likely enhancing root water uptake under drought conditions (Çakir, 2004). As crops transition into the reproductive phase, maize at silking and wheat at heading display heightened sensitivity of allocation coefficients to soil moisture. Under moderate to severe drought conditions (RAW < 60%), both maize and wheat exhibit decreasing trends in PL and YGR with increasing soil moisture (Fig. 2(b) and (e)), probably due to impaired plant capacity to maintain photosynthetic area and delay leaf senescence under water-limited conditions (Vadez et al., 2024). Notably, under mild drought to optimal water conditions (RAW = 60–85%), maize exhibits increasing PL and YGR with increasing moisture, indicating that appropriate irrigation during this stage effectively alleviates water stress and promotes greater allocation of photosynthates to foliage (Ma et al., 2025).

Importantly, maize and wheat also exhibit divergent photosynthate allocation patterns when exposed to water stress at the same developmental stage. During the reproductive transition phase, maize allocated more photosynthates to leaves under optimal water conditions, leading to increased LAI and prolonged leaf functionality,

which are critical for pollination and subsequent kernel formation (Ma et al., 2025). In contrast, wheat showed a continuous decline in PL, suggesting that photosynthates were increasingly diverted to the developing spike during anthesis stage, indicating a reduced dependence on leaf investment (Farooq et al., 2014). This divergence underscores an evolutionary trade-off between C4 and C3 crops in carbon use efficiency. Under water stress, maize prioritizes the protection of leaf function, whereas wheat ensures grain filling through strategic assimilate redistribution (Borrás et al., 2004; Smith et al., 2018). At maturity, maize exhibits reduced PR under drought because of premature root senescence, whereas PR increases under optimal or excessive soil moisture conditions (Fig. 2(c)). Inversely, wheat shows a simultaneous decline in both PR and YGR with increasing soil moisture (Fig. 2(f)). This finding indicates that, during the late grain-filling stage, wheat adopts a distinct photosynthate allocation strategy in which rapid root senescence promotes assimilate translocation from roots to grains, thereby supporting grain development.

In addition, excessive water availability also significantly affects the photosynthates allocation. At maize maturity, excessive soil moisture condition (RAW > 85%) resulted in higher YGR values than those observed under optimal water conditions. This response may be attributed to accelerated leaf senescence under excessive moisture conditions, which facilitates the remobilization of assimilates from vegetative tissues to grains. Excessive soil moisture reduces root aeration and increases respiratory losses, thereby weakening root activity (Shao et al., 2013; Herzog et al., 2015). Thus, excessive water supply can also disrupt the optimal allocation of photosynthates, ultimately impairing yield formation. For maize, both drought stress and excessive water conditions should be avoided during the silking and maturity stages to preserve leaf functionality and root activity. For wheat, careful water management is particularly important from jointing to heading to support proper spike differentiation and subsequent grain development.

## 4.3 Applicability and limitations of the optimized Agro-C model

### *4.3.1 Enhanced representation of water stress responses*

Crop models adopt various approaches to represent water stress. For instance, the DSSAT model constructs stress factors (TURFAC and SWFAC) based on the ratio of soil water supply to demand, applying them to processes such as photosynthesis, transpiration, leaf area development, and biomass accumulation (Jones et al., 2003; He et al., 2013). Although DSSAT effectively represents the effects of drought on photosynthesis and transpiration, photosynthate allocation is typically governed by fixed or stage-dependent allocation schemes, limiting the model's ability to simulate the dynamic redistribution of assimilates among plant organs. The APSIM model uses water stress factors to simulate the effects of water stress on root growth, leaf area expansion, and photosynthesis, while its modular and transparent framework enables its application across diverse cropping systems (Pasley et al., 2020; Githui et al., 2022; Monteleone et al., 2023). But the APSIM primarily relies on empirical functions to describe photosynthate allocation and does not explicitly represent the dynamic redistribution of assimilates among roots, leaves, and grains, limiting its ability to characterize carbon allocation at the organ level. The AquaCrop model uses threshold-based functions to simulate the effects of water stress on canopy expansion, stomatal conductance, leaf senescence, and harvest index, and generally performs well in simulating yield and water use efficiency under drought conditions. However, its representation of belowground processes remains relatively simplified, as root biomass is estimated mainly through adjustments to RSR, without explicitly accounting for root senescence or dynamic carbon allocation (Zhou et al., 2024; Fallah et al., 2025).

Compared with the aforementioned models, the optimized Agro-C model developed in this study provides a more mechanistic representation of crop responses to water stress by integrating a process-based root water uptake module with a dynamic photosynthate allocation scheme. Rather than relying solely on the RAW, the optimized model quantifies crop water status through root water uptake and water deficit ($\Delta W$), allowing carbon allocation (PR, PL, and YGR) to respond dynamically to both crop DVI and water availability. This enables the model to better represent

key physiological responses, such as enhanced root allocation and accelerated leaf senescence under water stress, thereby improving the simulation of AGB and BGB across a range of moisture conditions. Furthermore, because the optimized allocation scheme is constrained by observed biomass data and crop physiological characteristics, it provides a more physiologically realistic representation of organ-level carbon allocation than conventional approaches based on fixed allocation coefficients.

*4.3.2 Limitations of the optimized Agro-C model*

Despite the improved performance of the optimized Agro-C model, several limitations remain. In the original Agro-C framework, nitrogen cycling is coupled with crop carbon dynamics, with crop N uptake determined by N demand and N availability (Huang et al., 2009). Nitrogen availability subsequently influences photosynthetic carbon assimilation and biomass production. We retain the original representation of nitrogen processes, with site-specific fertilizer application rates incorporated as management inputs. Although the effects of nitrogen availability on crop growth are already represented in Agro-C, the present optimization specifically focuses on dynamically representing the effects of water availability on photosynthate allocation. However, the interactive effects of water and nitrogen on photosynthate allocation have not yet been explicitly incorporated into the current allocation scheme. Future work will therefore focus on elucidating how water and nitrogen jointly regulate organ-level photosynthate allocation and integrating these interactions into the model to better represent crop physiological responses under varying environmental and management conditions.

Moreover, the model still shows relatively lower accuracy in simulating BGB than AGB, suggesting that root growth processes are not yet fully represented. The current allocation scheme adjusts root carbon allocation primarily according to water conditions, while key root processes, such as root architecture, turnover, and carbon remobilization, are simplified. These processes, together with interactions among water availability, nitrogen, and temperature, are likely to influence root dynamics

and should be incorporated in future (Lynch et al., 2014; Calleja-Cabrera et al., 2022; Li et al., 2025). Furthermore, the current model can simulate different water conditions using site-specific irrigation inputs or relative available soil water, but it does not explicitly differentiate among irrigation strategies, including drip, sprinkler, and flood irrigation. To further improve the model, more detailed irrigation management practices, together with dynamic water–nitrogen interactions and root processes, should be incorporated to better capture crop physiological responses and belowground carbon dynamics under diverse environmental and management conditions.

## 5. Conclusion

This study incorporated water stress effects into crop carbon allocation by linking the root and leaf allocation coefficients (PR and PL) and the yellow-to-green leaf ratio (YGR) to soil moisture and DVI, thereby optimizing the Agro-C model. The optimized Agro-C model addresses limitations of fixed allocation rules by capturing stage-sensitive responses and dynamic shifts in allocation under drought and over-irrigation. Compared with the pre-optimized Agro-C model, the optimized Agro-C model demonstrated a substantial improvement in simulation accuracy, achieving $R^2$ values of 0.74–0.95 for AGB and 0.48–0.61 for BGB in validation datasets. Moreover, the optimized Agro-C model effectively captured biomass dynamics across a wide range of soil moisture conditions—from drought to excessive moisture—achieving $R^2$ values of 0.77–0.95 for AGB and 0.62–0.83 for BGB in maize and wheat, thereby demonstrating improved robustness and physiological fidelity. Nonetheless, the representation of root system architecture and turnover remains simplified, highlighting the need for further mechanistic refinement. Overall, the model presents a robust tool for simulating drought-induced carbon allocation strategies and can be applied in broader climate–agriculture interactions to inform sustainable water and carbon management strategies.

## Author contributions

WX: Conceptualization, Methodology, Formal analysis, Data curation, Visualization, Writing – original draft. WZ: Conceptualization, Writing – review & editing. YY: Investigation, Writing – review & editing. QZ: Conceptualization, Supervision, Project administration, Funding acquisition, Writing – review & editing.

**Competing interests**

The authors declare that they have no known competing financial interests or personal relationships that could have appeared to influence the work reported in this paper.

**Disclaimer. Publisher's note:**

Copernicus Publications remains neutral with regard to jurisdictional claims made in the text, published maps, institutional affiliations, or any other geographical representation in this paper. While Copernicus Publications makes every effort to include appropriate place names, the final responsibility lies with the authors.

**Code and data availability**

The code that supports the findings of this study is openly available in Zenodo at Xu et al. (2026; https://doi.org/10.5281/zenodo.19970992), reference number 19970992. All data used in this study are publicly available. Meteorological data for the crop growing period were obtained from *ERA5* (https://cds.climate.copernicus.eu/). The calibration data of the model are sourced from Duan (2020); Feng et al. (1997); Feng (2014); Ge et al. (2005); Ge et al. (2012); Gheysari et al. (2017); Jiang (2019); Li et al. (2010); Lu et al. (2020); Wang (2011); Wang et al. (2014); Wang (2014); Zhang (2023). The validation data of the model are sourced from Allard et al. (2013); Cai et al. (2017); Chen et al. (2021); Fang et al. (2017); Liu et al. (2017); Núñez et al. (2022); Pouri et al. (2019); Xu et al. (2020); Zhao et al. (2018); Zou et al. (2021).

**Acknowledgments**

This study was financially supported by the the National Key R&D Program of China (2022YFD1901604), National Natural Science Foundation of China

(42171064), and the Key Research and Development Program of Yunnan Province (202303AC100009).

## References


Ahuja, L., Ma, L., Timlin, D., Stockle, C., and Boote, K. J.: Current Water Deficit Stress Simulations in Selected Agricultural System Models, Response of Crops to Limited Water: Understanding and Modeling Water Stress Effects on Plant Growth Processes, https://doi.org/10.2134/advagricsystmodel1.c1, 2008.

Allard, V., Martre, P., and Le Gouis, J.: Genetic variability in biomass allocation to roots in wheat is mainly related to crop tillering dynamics and nitrogen status, European Journal of Agronomy, 46, 68–76, https://doi.org/10.1016/j.eja.2012.12.004, 2013.

Allen, R. G., Pereira, L. S., Smith, M., Raes, D., and Wright, J. L.: FAO-56 Dual Crop Coefficient Method for Estimating Evaporation from Soil and Application Extensions, J. Irrig. Drain Eng., 131, 2–13, https://doi.org/10.1061/(ASCE)0733-9437(2005)131:1(2), 2005.

Allen, R. G., Pruitt, W. O., Wright, J. L., Howell, T. A., Ventura, F., Snyder, R., Itenfisu, D., Steduto, P., Berengena, J., Yrisarry, J. B., Smith, M., Pereira, L. S., Raes, D., Perrier, A., Alves, I., Walter, I., and Elliott, R.: A recommendation on standardized surface resistance for hourly calculation of reference ETo by the FAO56 Penman-Monteith method, Agricultural Water Management, 81, 1–22, https://doi.org/10.1016/j.agwat.2005.03.007, 2006.

Asseng, S., Ewert, F., Rosenzweig, C., Jones, J. W., Hatfield, J. L., Ruane, A. C., Boote, K. J., Thorburn, P. J., Rötter, R. P., Cammarano, D., Brisson, N., Basso, B., Martre, P., Aggarwal, P. K., Angulo, C., Bertuzzi, P., Biernath, C., Challinor, A. J., Doltra, J., Gayler, S., Goldberg, R., Grant, R., Heng, L., Hooker, J., Hunt, L. A., Ingwersen, J., Izaurralde, R. C., Kersebaum, K. C., Müller, C., Naresh Kumar, S., Nendel, C., O'Leary, G., Olesen, J. E., Osborne, T. M., Palosuo, T., Priesack, E., Ripoche, D., Semenov, M. A., Shcherbak, I., Steduto, P., Stöckle, C., Stratonovitch, P., Streck, T., Supit, I., Tao, F., Travasso, M., Waha, K., Wallach, D., White, J. W., Williams, J. R., and Wolf, J.: Uncertainty in simulating wheat yields under climate change, Nature Clim Change, 3, 827–832, https://doi.org/10.1038/nclimate1916, 2013.

Bernacchi, C. J. and VanLoocke, A.: Terrestrial Ecosystems in a Changing Environment: A Dominant Role for Water, Annu. Rev. Plant Biol., 66, 599–622, https://doi.org/10.1146/annurev-arplant-043014-114834, 2015.

Bertheloot, J., Martre, P., and Andrieu, B.: Dynamics of Light and Nitrogen Distribution during Grain Filling within Wheat Canopy, Plant Physiol, 148, 1707–1720, https://doi.org/10.1104/pp.108.124156, 2008.

Boretti, A. and Rosa, L.: Reassessing the projections of the World Water Development Report, npj Clean Water, 2, 15, https://doi.org/10.1038/s41545-019-0039-9, 2019.

Borrás, L., Slafer, G. A., and Otegui, M. E.: Seed dry weight response to source–sink manipulations in wheat, maize and soybean: a quantitative reappraisal, Field Crops Research, 86, 131–146, https://doi.org/10.1016/j.fcr.2003.08.002, 2004.

Boyer, J. S.: Grain yields with limited water, Journal of Experimental Botany, 55, 2385–2394, https://doi.org/10.1093/jxb/erh219, 2004.

Cai, Q., Zhang, Y., Sun, Z., Zheng, J., Bai, W., Zhang, Y., Liu, Y., Feng, L., Feng, C., Zhang, Z.,

Yang, N., Evers, J. B., and Zhang, L.: Morphological plasticity of root growth under mild water stress increases water use efficiency without reducing yield in maize, Biogeosciences, 14, 3851–3858, https://doi.org/10.5194/bg-14-3851-2017, 2017.

Cai, G., Ahmed, M. A., Abdalla, M., and Carminati, A.: Root hydraulic phenotypes impacting water uptake in drying soils, Plant, Cell & Environment, 45, 650–663, https://doi.org/10.1111/pce.14259, 2022.

Çakir, R.: Effect of water stress at different development stages on vegetative and reproductive growth of corn, Field Crops Research, 89, 1–16, https://doi.org/10.1016/j.fcr.2004.01.005, 2004.

Calleja-Cabrera, J., Boter, M., Oñate-Sánchez, L., and Pernas, M.: Root Growth Adaptation to Climate Change in Crops, Front. Plant Sci., 11, https://doi.org/10.3389/fpls.2020.00544, 2020.

Chen, R., Xiong, X., and Cheng, W.: Root characteristics of spring wheat under drip irrigation and their relationship with aboveground biomass and yield, Sci Rep, 11, 4913, https://doi.org/10.1038/s41598-021-84208-7, 2021.

Chen, Z., Niu, Y., Zhao, R., Han, C., Han, H., and Luo, H.: The combination of limited irrigation and high plant density optimizes canopy structure and improves the water use efficiency of cotton, Agricultural Water Management, 218, 139–148, https://doi.org/10.1016/j.agwat.2019.03.037, 2019.

Cook, B. I., Smerdon, J. E., Seager, R., and Coats, S.: Global warming and 21st century drying, Clim Dyn, 43, 2607–2627, https://doi.org/10.1007/s00382-014-2075-y, 2014.

Dai, A.: Increasing drought under global warming in observations and models, Nature Clim Change, 3, 52–58, https://doi.org/10.1038/nclimate1633, 2013.

Duan, W.: Dynamic Response of Root-shoot Growth of Summer Maize to Soil Moisture under Deficit Irrigation, Northwest A&F University in Partial Fulfillment of the Requirements, 2022.

van Diepen, C. a., Wolf, J., van Keulen, H., and Rappoldt, C.: WOFOST: a simulation model of crop production, Soil Use and Management, 5, 16–24, https://doi.org/10.1111/j.1475-2743.1989.tb00755.x, 1989.

Dodd, I. C., Egea, G., Watts, C. W., and Whalley, W. R.: Root water potential integrates discrete soil physical properties to influence ABA signalling during partial rootzone drying, Journal of Experimental Botany, 61, 3543–3551, https://doi.org/10.1093/jxb/erq195, 2010.

Effah, Z., Li, L., Xie, J., Karikari, B., Wang, J., Zeng, M., Wang, L., Boamah, S., and Padma Shanthi, J.: Post-anthesis Relationships Between Nitrogen Isotope Discrimination and Yield of Spring Wheat Under Different Nitrogen Levels, Front. Plant Sci., 13, https://doi.org/10.3389/fpls.2022.859655, 2022.

Fallah, M., Rasulov, A., Ekambaram, Y., Khudayberganov, K., Devi Kosuru, S. n. v. j., and Ghate, A. D.: Simulating Plant Growth Under Water Stress Using the AquaCrop Model, Natural and Engineering Sciences, 10, 447–458, https://doi.org/10.28978/nesciences.1763853, 2025.

Fang, Y., Du, Y., Wang, J., Wu, A., Qiao, S., Xu, B., Zhang, S., Siddique, K.H.M., Chen, Y.: Moderate Drought Stress Affected Root Growth and Grain Yield in Old, Modern and Newly Released Cultivars of Winter Wheat, Front. Plant Sci. 8, 672, https://doi.org/10.3389/fpls.2017.00672, 2017.

Farooq, M., Wahid, A., Kobayashi, N., Fujita, D., and Basra, S. M. A.: Plant drought stress: effects, mechanisms and management, Agron. Sustain. Dev., 29, 185–212, https://doi.org/10.1051/agro:2008021, 2009.

Farooq, M., Hussain, M., and Siddique, K. H. M.: Drought Stress in Wheat during Flowering and Grain-filling Periods, Critical Reviews in Plant Sciences, 33, 331–349, https://doi.org/10.1080/07352689.2014.875291, 2014.

Feng, G., Luo, Y.: Simulation on Functional Equilibrium of Winter Wheat Root and Shoot under Different Soil Water Regimes, Acta Ecologica Sinica 19, 1, 1999.

Feng, H., Tan, X., Bi, Jian.: Study on the Root Distribution and Root Characteristics of Winter Wheat under Different Soil and Water Conditions, Journal of Anhui Agri. Sci. 2013, 41( 35) : 13465 - 13467,13471, 2013.

Field, C. B., Randerson, J. T., and Malmström, C. M.: Global net primary production: Combining ecology and remote sensing, Remote Sensing of Environment, 51, 74–88, https://doi.org/10.1016/0034-4257(94)00066-V, 1995.

Ge, T., Sui, F., Li, J., Lv, Y., Zhou, G.: Effects of Drought on Growth of Root and Shoot of Summer Maize, Chinese Agricultural Science Bulletin 21, 1, 2005.

Ge, T., Sui, F., Bai, L., Tong, C., and Sun, N.: Effects of water stress on growth, biomass partitioning, and water-use efficiency in summer maize (Zea mays L.) throughout the growth cycle, Acta Physiol Plant, 34, 1043–1053, https://doi.org/10.1007/s11738-011-0901-y, 2012.

Gheysari, M., Sadeghi, S.-H., Loescher, H. W., Amiri, S., Zareian, M. J., Majidi, M. M., Asgarinia, P., and Payero, J. O.: Comparison of deficit irrigation management strategies on root, plant growth and biomass productivity of silage maize, Agricultural Water Management, 182, 126–138, https://doi.org/10.1016/j.agwat.2016.12.014, 2017.

Githui, F., Beverly, C., Aiad, M., McCaskill, M., Liu, K., and Harrison, M. T.: Modelling Waterlogging Impacts on Crop Growth: A Review of Aeration Stress Definition in Crop Models and Sensitivity Analysis of APSIM, International Journal of Plant Biology, 13, 180–200, https://doi.org/10.3390/ijpb13030017, 2022.

Gupta, A., Rico-Medina, A., and Caño-Delgado, A. I.: The physiology of plant responses to drought, Science, 368, 266–269, https://doi.org/10.1126/science.aaz7614, 2020.

Hafner, B. D., Hesse, B. D., Bauerle, T. L., and Grams, T. E. E.: Water potential gradient, root conduit size and root xylem hydraulic conductivity determine the extent of hydraulic redistribution in temperate trees, Functional Ecology, 34, 561–574, https://doi.org/10.1111/1365-2435.13508, 2020.

Hammer, G. L., Van Oosterom, E., McLean, G., Chapman, S. C., Broad, I., Harland, P., and Muchow, R. C.: Adapting APSIM to model the physiology and genetics of complex adaptive traits in field crops, Journal of Experimental Botany, 61, 2185–2202,

https://doi.org/10.1093/jxb/erq095, 2010.

He, J., Cai, H., and Bai, J.: Irrigation scheduling based on CERES-Wheat model for spring wheat production in the Minqin Oasis in Northwest China, Agricultural Water Management, 128, 19–31, https://doi.org/10.1016/j.agwat.2013.06.010, 2013.

Herzog, M., Striker, G. G., Colmer, T. D., and Pedersen, O.: Mechanisms of waterlogging tolerance in wheat – a review of root and shoot physiology, Plant, Cell & Environment, 39, 1068–1086, https://doi.org/10.1111/pce.12676, 2016.

Hijmans, R. J., Lens, I. M. G.-, and Diepen, C. A. van: WOFOST 6.0 : user's guide for the WOFOST 6.0 crop growth simulation model, 1994.

Hu, J., Zhao, X., Gu, L., Liu, P., Zhao, B., Zhang, J., and Ren, B.: The effects of high temperature, drought, and their combined stresses on the photosynthesis and senescence of summer maize, Agricultural Water Management, 289, 108525, https://doi.org/10.1016/j.agwat.2023.108525, 2023.

Hu, T., Zhang, X., Khanal, S., Wilson, R., Leng, G., Toman, E. M., Wang, X., Li, Y., and Zhao, K.: Climate change impacts on crop yields: A review of empirical findings, statistical crop models, and machine learning methods, Environmental Modelling & Software, 179, 106119, https://doi.org/10.1016/j.envsoft.2024.106119, 2024.

Huang, Y., Yu, Y., Zhang, W., Sun, W., Liu, S., Jiang, J., Wu, J., Yu, W., Wang, Y., and Yang, Z.: Agro-C: A biogeophysical model for simulating the carbon budget of agroecosystems, Agricultural and Forest Meteorology, 149, 106–129, https://doi.org/10.1016/j.agrformet.2008.07.013, 2009.

Jiang, P., Cai, F., Zhao, Z.Q., Meng, Y., Gao, L.Y., and Zhao, T.H.: Physiological and Dry Matter Characteristics of Spring Maize in Northeast China under Drought Stress, Water, 10, 1561, https://doi.org/10.3390/w10111561, 2018.

Jiang, P.: Northeast Corn Material Production and Root Water Absorption Study on the Response of Water Stress, Shenyang Agricultural University, 2019.

Jones, J. W., Hoogenboom, G., Porter, C. H., Boote, K. J., Batchelor, W. D., Hunt, L. A., Wilkens, P. W., Singh, U., Gijsman, A. J., and Ritchie, J. T.: The DSSAT cropping system model, European Journal of Agronomy, 18, 235–265, https://doi.org/10.1016/S1161-0301(02)00107-7, 2003.

Kang, J., Peng, Y., and Xu, W.: Crop Root Responses to Drought Stress: Molecular Mechanisms, Nutrient Regulations, and Interactions with Microorganisms in the Rhizosphere, Int J Mol Sci, 23, 9310, https://doi.org/10.3390/ijms23169310, 2022.

Kang, M.-S., Srivastava, P., Song, J.-H., Park, J., Her, Y., Kim, S. M., and Song, I.: Development of a Component-Based Modeling Framework for Agricultural Water-Resource Management, Water, 8, 351, https://doi.org/10.3390/w8080351, 2016.

Keating, B. A., Carberry, P. S., Hammer, G. L., Probert, M. E., Robertson, M. J., Holzworth, D., Huth, N. I., Hargreaves, J. N. G., Meinke, H., Hochman, Z., McLean, G., Verburg, K., Snow, V., Dimes, J. P., Silburn, M., Wang, E., Brown, S., Bristow, K. L., Asseng, S., Chapman, S., McCown, R. L., Freebairn, D. M., and Smith, C. J.: An overview of APSIM, a model

designed for farming systems simulation, European Journal of Agronomy, 18, 267–288, https://doi.org/10.1016/S1161-0301(02)00108-9, 2003.

Khatun, M., Sarkar, S., Era, F. M., Islam, A. K. M. M., Anwar, M. P., Fahad, S., Datta, R., and Islam, A. K. M. A.: Drought Stress in Grain Legumes: Effects, Tolerance Mechanisms and Management, Agronomy, 11, 2374, https://doi.org/10.3390/agronomy11122374, 2021.

Lesk, C., Rowhani, P., and Ramankutty, N.: Influence of extreme weather disasters on global crop production, Nature, 529, 84–87, https://doi.org/10.1038/nature16467, 2016.

Li, H., Qiu, J., Wang, L., and Yang, L.: Advance in a terrestrial biogeochemical model—DNDC model, Acta Ecologica Sinica, 31, 91–96, https://doi.org/10.1016/j.chnaes.2010.11.006, 2011.

Li, T., Hasegawa, T., Yin, X., Zhu, Y., Boote, K., Adam, M., Bregaglio, S., Buis, S., Confalonieri, R., Fumoto, T., Gaydon, D., Marcaida III, M., Nakagawa, H., Oriol, P., Ruane, A. C., Ruget, F., Singh, B.-, Singh, U., Tang, L., Tao, F., Wilkens, P., Yoshida, H., Zhang, Z., and Bouman, B.: Uncertainties in predicting rice yield by current crop models under a wide range of climatic conditions, Global Change Biology, 21, 1328–1341, https://doi.org/10.1111/gcb.12758, 2015.

Li, Y., Wang, Q., Gao, S., Wang, X., He, A., and He, P.: Effects of Water–Nitrogen Coupling on Root Distribution and Yield of Summer Maize at Different Growth Stages, Plants, 14, 1278, https://doi.org/10.3390/plants14091278, 2025.

Lidon, Z.: An overview on drought induced changes in plant growth, water relationsand photosynthesis, Emir. J. Food Agric, 24, 57, https://doi.org/10.9755/ejfa.v24i1.10599, 2012.

Liu, Z., Zhu, K., Dong, S., Liu, P., Zhao, B., and Zhang, J.: Effects of integrated agronomic practices management on root growth and development of summer maize, European Journal of Agronomy, 84, 140–151, https://doi.org/10.1016/j.eja.2016.12.006, 2017.

Lu, H., Xia, Z., Fu, Y., Wang, Q., Xue, J., and Chu, J.: Response of Soil Temperature, Moisture, and Spring Maize (Zea mays L.) Root/Shoot Growth to Different Mulching Materials in Semi-Arid Areas of Northwest China, Agronomy, 10, 453, https://doi.org/10.3390/agronomy10040453, 2020.

Lynch, J. P., Chimungu, J. G., and Brown, K. M.: Root anatomical phenes associated with water acquisition from drying soil: targets for crop improvement, J Exp Bot, 65, 6155–6166, https://doi.org/10.1093/jxb/eru162, 2014.

Ma, Y., Ren, J., Yang, S., Ding, R., Du, T., Kang, S., and Tong, L.: Enhancing maize yield and water productivity through coordinated root-shoot growth under mild water stress in dense planting, Field Crops Research, 323, 109786, https://doi.org/10.1016/j.fcr.2025.109786, 2025.

Manghwar, H., Hussain, A., Alam, I., Khoso, M. A., Ali, Q., and Liu, F.: Waterlogging stress in plants: Unraveling the mechanisms and impacts on growth, development, and productivity, Environmental and Experimental Botany, 224, 105824, https://doi.org/10.1016/j.envexpbot.2024.105824, 2024.

McCown, R. L., Hammer, G. L., Hargreaves, J. N. G., Holzworth, D. P., and Freebairn, D. M.:

APSIM: a novel software system for model development, model testing and simulation in agricultural systems research, Agricultural Systems, 50, 255–271, https://doi.org/10.1016/0308-521X(94)00055-V, 1996.

Monteleone, B., Borzí, I., Arosio, M., Cesarini, L., Bonaccorso, B., and Martina, M.: Modelling the response of wheat yield to stage-specific water stress in the Po Plain, Agricultural Water Management, 287, 108444, https://doi.org/10.1016/j.agwat.2023.108444, 2023.

Munns, R. and Tester, M.: Mechanisms of Salinity Tolerance, Annu. Rev. Plant Biol., 59, 651–681, https://doi.org/10.1146/annurev.arplant.59.032607.092911, 2008.

Núñez, A., Ball, R., and Schipanski, M.: Plant and soil microbial responses to irrigation retirement in semiarid cropping systems, Environ. Res. Commun., 4, 035004, https://doi.org/10.1088/2515-7620/ac59c3, 2022.

Novák, V., Hurtalová, T., and Matejka, F.: Predicting the effects of soil water content and soil water potential on transpiration of maize, Agricultural Water Management, 76, 211–223, https://doi.org/10.1016/j.agwat.2005.01.009, 2005.

Oktem, A.: Effect of water shortage on yield, and protein and mineral compositions of drip-irrigated sweet corn in sustainable agricultural systems, Agricultural Water Management, 95, 1003–1010, https://doi.org/10.1016/j.agwat.2008.03.006, 2008.

Palta, J. A., Kobata, T., Turner, N. C., and Fillery, I. R.: Remobilization of Carbon and Nitrogen in Wheat as Influenced by Postanthesis Water Deficits, Crop Science, 34, 118–124, https://doi.org/10.2135/cropsci1994.0011183X003400010021x, 1994.

Pasley, H. R., Huber, I., Castellano, M. J., and Archontoulis, S. V.: Modeling Flood-Induced Stress in Soybeans, Front. Plant Sci., 11, 62, https://doi.org/10.3389/fpls.2020.00062, 2020.

Pouri, K., Mardeh, A. S.-S., Sohrabi, Y., and Soltani, A.: Crop phenotyping for wheat yield and yield components against drought stress, Cereal Research Communications, 47, 383–393, https://doi.org/10.1556/0806.47.2019.05, 2019.

Priestley, C. H. B. and Taylor, R. J.: On the Assessment of Surface Heat Flux and Evaporation Using Large-Scale Parameters, 1972.

Protto, V., Bauget, F., Rishmawi, L., Nacry, P., and Maurel, C.: Primary, seminal and lateral roots of maize show type-specific growth and hydraulic responses to water deficit, Plant Physiology, 194, 2564–2579, https://doi.org/10.1093/plphys/kiad675, 2024.

Rishmawi, L., Bauget, F., Protto, V., Bauland, C., Nacry, P., and Maurel, C.: Natural variation of maize root hydraulic architecture underlies highly diverse water uptake capacities, Plant Physiology, 192, 2404–2418, https://doi.org/10.1093/plphys/kiad213, 2023.

Ritchie, J. T.: Soil water balance and plant water stress, in: Understanding Options for Agricultural Production, edited by: Tsuji, G. Y., Hoogenboom, G., and Thornton, P. K., Springer Netherlands, Dordrecht, 41–54, https://doi.org/10.1007/978-94-017-3624-4_3, 1998.

Saseendran, S. a., Ahuja, L. r., Ma, L., and Trout, T. j.: Modeling for Best Management of the Effects of Irrigation Frequencies, Initial Water, and Nitrogen on Corn, in: Practical

Applications of Agricultural System Models to Optimize the Use of Limited Water, John Wiley & Sons, Ltd, 25–52, https://doi.org/10.2134/advagricsystmodel5.c2, 2014.

Saxton, K. E. and Rawls, W. J.: Soil Water Characteristic Estimates by Texture and Organic Matter for Hydrologic Solutions, Soil Science Soc of Amer J, 70, 1569–1578, https://doi.org/10.2136/sssaj2005.0117, 2006.

Seleiman, M. F., Al-Suhaibani, N., Ali, N., Akmal, M., Alotaibi, M., Refay, Y., Dindaroglu, T., Abdul-Wajid, H. H., and Battaglia, M. L.: Drought Stress Impacts on Plants and Different Approaches to Alleviate Its Adverse Effects, Plants, 10, 259, https://doi.org/10.3390/plants10020259, 2021.

Shao, G. C., Lan, J. J., Yu, S. E., Liu, N., Guo, R. Q., and She, D. L.: Photosynthesis and growth of winter wheat in response to waterlogging at different growth stages, Photosynthetica, 51, 429–437, https://doi.org/10.1007/s11099-013-0039-9, 2013.

Smith, M. R., Rao, I. M., and Merchant, A.: Source-Sink Relationships in Crop Plants and Their Influence on Yield Development and Nutritional Quality, Front. Plant Sci., 9, https://doi.org/10.3389/fpls.2018.01889, 2018.

Steduto, P., Hsiao, T. C., Raes, D., and Fereres, E.: AquaCrop—The FAO Crop Model to Simulate Yield Response to Water: I. Concepts and Underlying Principles, Agronomy Journal, 101, 426–437, https://doi.org/10.2134/agronj2008.0139s, 2009.

Stöckle, C. O., Donatelli, M., and Nelson, R.: CropSyst, a cropping systems simulation model, European Journal of Agronomy, 18, 289–307, https://doi.org/10.1016/S1161-0301(02)00109-0, 2003.

Tsuji, G. Y.: Understanding Options for Agricultural Production, 1st ed., Springer Netherlands, Dordrecht, 1 pp., 1998.

Vadez, V., Grondin, A., Chenu, K., Henry, A., Laplaze, L., Millet, E. J., and Carminati, A.: Crop traits and production under drought, Nat Rev Earth Environ, 5, 211–225, https://doi.org/10.1038/s43017-023-00514-w, 2024.

van Genuchten, M. T.: A closed-form equation for predicting the hydraulic conductivity of unsaturated soils, Soil Science Society of America Journal, 44(5), 892–898, https://doi.org/10.2136/sssaj1980.03615995004400050002x, 1980.

Vicente-Serrano, S. M., Peña-Angulo, D., Beguería, S., Domínguez-Castro, F., Tomás-Burguera, M., Noguera, I., Gimeno-Sotelo, L., and El Kenawy, A.: Global drought trends and future projections, Phil. Trans. R. Soc. A., 380, 20210285, https://doi.org/10.1098/rsta.2021.0285, 2022.

Wang, C., Liu, W., Li, Q., Ma, D., Lu, H., Feng, W., Xie, Y., Zhu, Y., and Guo, T.: Effects of different irrigation and nitrogen regimes on root growth and its correlation with above-ground plant parts in high-yielding wheat under field conditions, Field Crops Research, 165, 138–149, https://doi.org/10.1016/j.fcr.2014.04.011, 2014.

Wang, G., Huang, Y., Zhang, W., Yu, Y., and Sun, W.: Quantifying carbon input for targeted soil organic carbon sequestration in China's croplands, Plant Soil, 394, 57–71, https://doi.org/10.1007/s11104-015-2508-3, 2015.

Wang, L., Liu, X., Liu, X., Bao, X., Zhang, X., Yin, B., Wang, W., Wang, Y., and Zhen, W.: Effects of spring limited irrigation on grain yield and root characteristics of winter wheat in groundwater-overexploitation areas in the North China Plain, Agricultural Water Management, 294, 108729, https://doi.org/10.1016/j.agwat.2024.108729, 2024.

Wang, Y.:. Study on the relationship among root system and shoot dry matter accumulation and yield from winter wheat under different cultivation and management modes, Henan Agricultural University, 2011

Wang, Y.: Studies on Formation of Root Configuration and Its Relationships to Utilization of Water and Nitrogen Fertilizers and Grain Yield in Winter Wheat (Triticum aestivum L.) under Different Cultivation Management Patterns, Henan Agricultural University, 2014.

Wolf, J.: Calibration of WOFOST crop growth simulation model for use within CGMS, n.d.

Xu, H., Vandecasteele, B., Maenhout, P., Pannecoucque, J., De Neve, S., and Sleutel, S.: Maize root biomass and architecture depend on site but not on variety: Consequences for prediction of C inputs and spread in topsoil based on root-to-shoot ratios, European Journal of Agronomy, 119, 126121, https://doi.org/10.1016/j.eja.2020.126121, 2020.

Xu, W., Zhang, W., Yu, Y., Sun, W., Yu, L., Shang, D., Xue, C., and Zhang, Q.: Response of crop photosynthetic product allocation under different water supply conditions: A global synthetic analysis, Field Crops Research, 333, 110104, https://doi.org/10.1016/j.fcr.2025.110104, 2025.

Xu, W., Zhang, W., Yu, Y., & Zhang, Q.: Optimization code of Agro-C water module and photosynthetic product allocation module. In Improving photo (1.0), Zenodo. https://doi.org/10.5281/zenodo.19970992, 2026

Xue, Q., Zhu, Z., Musick, J. T., Stewart, B. A., and Dusek, D. A.: Root growth and water uptake in winter wheat under deficit irrigation, Plant and Soil, 257, 151–161, https://doi.org/10.1023/A:1026230527597, 2003.

Yan, Z., Liu, Y., Gao, S., Yang, H., Feng, D., Gao, K., Ming, B., Wang, K., Hou, P., Li, S., and Xie, R.: Water management mitigates drought stress effects on maize leaf senescence and post-anthesis dry matter accumulation, Agricultural Water Management, 318, 109709, https://doi.org/10.1016/j.agwat.2025.109709, 2025.

Yang, Y., Ma, X., Yan, L., Li, Y., Wei, S., Teng, Z., Zhang, H., Tang, W., Peng, S., and Li, Y.: Soil–root interface hydraulic conductance determines responses of photosynthesis to drought in rice and wheat, Plant Physiology, 194, 376–390, https://doi.org/10.1093/plphys/kiad498, 2023.

Yu, Y., Huang, Y., and Zhang, W.: Changes in rice yields in China since 1980 associated with cultivar improvement, climate and crop management, Field Crops Research, 136, 65–75, https://doi.org/10.1016/j.fcr.2012.07.021, 2012.

Zeitoun, M., Lankford, B., Krueger, T., Forsyth, T., Carter, R., Hoekstra, A. Y., Taylor, R., Varis, O., Cleaver, F., Boelens, R., Swatuk, L., Tickner, D., Scott, C. A., Mirumachi, N., and Matthews, N.: Reductionist and integrative research approaches to complex water security policy challenges, Global Environmental Change, 39, 143–154, https://doi.org/10.1016/j.gloenvcha.2016.04.010, 2016.

Zhao, J., Xue, Q., Jessup, K. E., Hou, X., Hao, B., Marek, T. H., Xu, W., Evett, S. R., O'Shaughnessy, S. A., and Brauer, D. K.: Shoot and root traits in drought tolerant maize (Zea mays L.) hybrids, Journal of Integrative Agriculture, 17, 1093–1105, https://doi.org/10.1016/S2095-3119(17)61869-0, 2018.

Zhang, Q., Zhang, W., Li, T., Sun, W., Yu, Y., and Wang, G.: Projective analysis of staple food crop productivity in adaptation to future climate change in China, Int J Biometeorol, 61, 1445–1460, https://doi.org/10.1007/s00484-017-1322-4, 2017.

Zhang, X.: Effects of Different Water-Nitrogen Treatments on Root Growth and the Accumulation and Translocation of Aboveground Dry Matter together with Yield in Wheat, Henan Agricultural University, 2023.

Zhou, D., Wang, H., Wang, X., Wang, F., Zhang, J., and Ma, D.: Evaluation of AquaCrop's Ability to Simulate Water Stress Based on 2-Year Case Study of Maize Crop, Agronomy, 14, 354, https://doi.org/10.3390/agronomy14020354, 2024.

Zlatev, Z. and Lidon, F.: An overview on drought induced changes in plant growth, water relations and photosynthesis, Emirates Journal of Food and Agriculture, 24, 2012

Zou, Y., Saddique, Q., Ali, A., Xu, J., Khan, M. I., Qing, M., ... & Siddique, K. H.: Deficit irrigation improves maize yield and water use efficiency in a semi-arid environment, Agricultural Water Management, 243, 106483, 2021.